



HAL
open science

Numerical simulation of complex fluid drying in a Hele-Shaw cell

Ching Hsueh, Frédéric Doumenc, Béatrice Guerrier

► **To cite this version:**

Ching Hsueh, Frédéric Doumenc, Béatrice Guerrier. Numerical simulation of complex fluid drying in a Hele-Shaw cell. *The European Physical Journal. Special Topics*, 2013, 219 (1), pp.51-57. 10.1140/epjst/e2013-01780-8 . hal-04372323

HAL Id: hal-04372323

<https://hal.science/hal-04372323>

Submitted on 4 Jan 2024

HAL is a multi-disciplinary open access archive for the deposit and dissemination of scientific research documents, whether they are published or not. The documents may come from teaching and research institutions in France or abroad, or from public or private research centers.

L'archive ouverte pluridisciplinaire **HAL**, est destinée au dépôt et à la diffusion de documents scientifiques de niveau recherche, publiés ou non, émanant des établissements d'enseignement et de recherche français ou étrangers, des laboratoires publics ou privés.

Numerical Simulation of Complex Fluid Drying in a Hele-Shaw Cell

Ching Hsueh¹, Frédéric Doumenc^{1,a} and Béatrice Guerrier¹

UPMC Univ Paris 06, Univ Paris-Sud, CNRS, UMR 7608, Lab. FAST, Bât 502, Campus Universitaire, Orsay, F-91405, France

Abstract. A 2D model is currently under development to describe the flow and concentration fields inside a Hele-Shaw cell with evaporation for a receding meniscus (dip-coating-like configuration). An original approach is proposed to address the difficult problem of the boundary conditions close to the contact line. The model is used to study the deposit thickness as a function of some process parameters.

1 Introduction

Dip-coating is a widely used industrial coating process, with complex coupling between hydrodynamics, mass transfer and evaporation, especially close to the contact line. Through various experimental and theoretical studies, it is now well established that different regimes appear depending on the Capillary number $Ca \equiv \mu V / \gamma$ (μ being the dynamic viscosity, V the substrate velocity, and γ the surface tension) [1–6]. At small Capillary number, viscous forces are strong enough to drag a liquid film whose thickness increases as $V^{2/3}$ (classical Landau-Levich regime). For even smaller Capillary numbers, another regime dominated by evaporation at the meniscus is encountered, characterized by a deposit thickness proportional to V^{-1} . Our objective is to build a hydrodynamic model of a dip-coating-like experiment (see reference [4]), in order to investigate the relation between the flow and the concentration field in the meniscus on one hand, and the deposit thickness on the other hand. In the present study which is a first step towards a more complete model of the process, we only take into account the flow driven by the substrate movement and the solvent evaporation. The free convection induced by buoyancy and/or Marangoni effect, which has been observed in the experiments, is temporarily disregarded. We focus on the difficult problem of the boundary conditions close to the contact line. An original approach based on lubrication approximation is presented, which avoids addressing stress and evaporative flux singularities, but still allows the prediction of the deposit thickness. This model may be viewed as the definition of the basic state for a future study of hydrodynamic instabilities in dip-coating processes.

^a e-mail: frederic.doumenc@upmc.fr

2 Model

2.1 Geometry and assumptions

The model is based on experiments performed in a dip-coating-like set-up [4]. The device is made of two parallel glass plates separated by a gap d which are vertically immersed in a reservoir filled with a solution of solute volume fraction ϕ_{p0} . Once the plates are immersed in the solution, there is a spontaneous capillary rise in the Hele-Shaw cell. The reservoir is then emptied at a constant pumping rate so that the position of the contact line decreases at velocity V . In our model, we consider the reverse equivalent configuration, i.e. the wall is moving upward with velocity V , while the meniscus is fixed. The mean evaporation velocity on the meniscus, v_{ev} , is controlled by a vertical air flow blown between the two glass plates, at a given temperature and humidity. A 2D domain is used to simulate the experimental set-up (figure 1). The total height H is large enough to get a fully developed flow at the bottom. The meniscus is assumed circular with radius R . Indeed, deformation induced by substrate motion or evaporation is located in the vicinity of the tip which is truncated in our model (cf. description below). For the complete wetting configuration considered in this study, $R = d/2 = 0.5mm$.

In the first step presented here, several simplifying assumptions have been made. Buoyancy, Marangoni effect and inertia are neglected. The solution density ρ is a constant (same specific partial volume for the solvent and solute, so that the solvent (or the solute) mass and volume fractions are identical). The problem is isothermal. To capture the basic characteristics of the local evaporation rate, i.e. a strong increase at the meniscus tip [6], the following expression is used: $j(m/s) = J_0/\sqrt{D_{tip}}$, where $D_{tip} = H - y$ is the distance to the tip of the contact line along the vertical axis. Note that this expression for the local evaporation rate is an approximation valid at the tip vicinity of the relation first suggested by Deegan *et al.* [7] for a sessile droplet. In this work, it is extended to the entire free surface, as a first step. $J_0(m^{3/2}s^{-1})$ is a constant deduced from the experimental value of v_{ev} (m/s)¹. v_{ev} is obtained from preliminary experiments with pure water [4]. The dependence of the evaporation flux on the solute concentration is neglected.

Since the evaporation rate diverges at the tip, we define the truncated region shown in figure 1 by cutting off a small tip region whose height is α and width is δ . The flow is assumed to be incompressible and the fluid to be Newtonian. Under these assumptions mass conservation and Stokes equations read in vector form:

$$\nabla \cdot \mathbf{v} = 0, \quad -\nabla P + \nabla \cdot (\mu \nabla \mathbf{v} + \mu \nabla^t \mathbf{v}) = 0, \quad (1)$$

where $\mathbf{v} = u\mathbf{i} + v\mathbf{j}$ is the velocity field, μ is the viscosity (assumed constant in the following) and P is the pressure. The mass balance for the solute reads:

$$\mathbf{v} \cdot \nabla \phi_p = D \nabla^2 \phi_p, \quad (2)$$

where ϕ_p is the volume fraction of solute and D is the binary diffusion coefficient.

2.2 Boundary conditions

We assume no slip and impermeable boundary conditions at Boundary 1 and symmetry conditions at Boundary 3 (see figure 1). At $y = 0$ (Boundary 2) we consider a

¹ $v_{ev} = \frac{1}{R} \int_0^{\pi R/2} \frac{J_0}{\sqrt{H-y}} ds = J_0 \int_{H-R}^H \frac{dy}{\sqrt{(H-y)(R-H+y)(R+H-y)}}$ with ds being an element of the free surface.

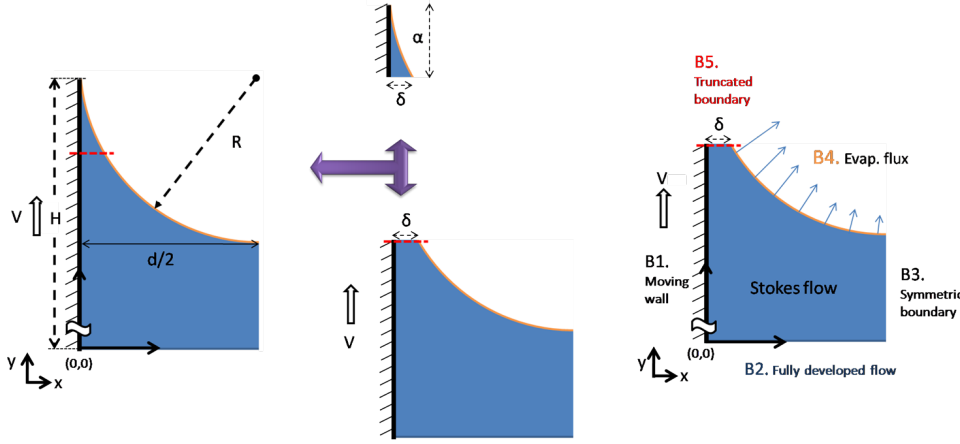


Fig. 1. Sketch of the numerical domain and boundary conditions.

fully developed flow. The concentration is assumed to be the bulk concentration ϕ_{p0} for the inflow, and diffusion is neglected for the outflow:

$$u = 0, \quad \frac{\partial v}{\partial y} = 0, \quad (3)$$

$$\mathbf{v} \cdot \mathbf{j} > 0 \implies \phi_p = \phi_{p0} \text{ (inflow)}, \quad \mathbf{v} \cdot \mathbf{j} < 0 \implies \frac{\partial \phi_p}{\partial y} = 0 \text{ (outflow)}. \quad (4)$$

Along the meniscus (Boundary 4), a first equation is the stress-free condition. Other equations are related to the evaporation flux (with a volatile solvent and a non-volatile solute). With the assumption of a constant density for the solution we obtain

$$\frac{\partial u_t}{\partial n} + \frac{\partial u_n}{\partial t} = 0, \quad \mathbf{J}_p \cdot \mathbf{n} = 0, \quad u_n = j, \quad j = \frac{J_0}{\sqrt{H-y}}, \quad (5)$$

where $\mathbf{v} = u_n \mathbf{n} + u_t \mathbf{t}$, \mathbf{t} and \mathbf{n} are the tangential and normal unit vectors along the meniscus, respectively. \mathbf{J}_p is the solute mass flux ².

The last boundary (Boundary 5 at $y = H - \alpha$) is the most intricate. We truncate the meniscus at a small distance α from the contact line. The resulting boundary has a width δ (see figure 1). In this region the flow is quasi-parallel to the moving wall (small slope approximation) and the lubrication approximation applies. Moreover, δ is assumed small enough to neglect the variation of the solute volume fraction along the boundary. The simplified Stokes equations read

$$\frac{\partial P}{\partial x} = 0, \quad \frac{\partial P}{\partial y} = \mu \frac{\partial^2 v}{\partial x^2}. \quad (6)$$

Using the no-slip condition at $x = 0$, the zero shear stress condition at $x = \delta$, and with \bar{V}_{tip} the mean velocity y -component along the boundary B5 ($\bar{V}_{tip} = 1/\delta \int_0^\delta v(x, y) dx$), integration of the above equation leads to

$$v(x, y) = \frac{3}{\delta} (\bar{V}_{tip} - V) x \left(1 - \frac{x}{2\delta}\right) + V. \quad (7)$$

² with the assumption of a constant solution density, $\mathbf{J}_p = \Phi_p \rho \mathbf{v} - \rho D \nabla \Phi_p$

Considering Eq. (1) and the local mass balance (with the assumption of a constant density ρ for the solution), we obtain

$$u(x, y) = [\bar{V}_{tip} \frac{d\delta}{dy} (3\delta - 2x) + V \frac{d\delta}{dy} (2x - 3\delta) + \delta \frac{d\bar{V}_{tip}}{dy} (x - 3\delta)] \frac{x^2}{2\delta^3} \quad (8)$$

$$\text{with } \delta(y) = \frac{(H - y)^2}{2R}, \quad \frac{d\delta}{dy} = \frac{y - H}{R}, \quad \frac{d\bar{V}_{tip}}{dy} = -\frac{1}{\delta} \left[j(y) + \bar{V}_{tip} \frac{d\delta}{dy} \right]. \quad (9)$$

Equations (7) and (8) estimated at $y = H - \alpha$ yield the hydrodynamic boundary conditions. Finally, assuming that B5 is an outlet ($\mathbf{v} \cdot \mathbf{j} \geq 0$ over the whole boundary), we impose $\partial\phi_p/\partial y = 0$ for the concentration field. This approximation is expected to induce an error only in a small region over a length of order $\frac{D}{\bar{V}_{tip}}$ close to the boundary.

The value \bar{V}_{tip} is unknown and is obtained by successive trials in the following way. For a given value of \bar{V}_{tip} , the above model is used to obtain the concentration field in the entire computational domain and in particular, on the boundary B5. We first check that the concentration is nearly uniform on B5 (variations are typically less than 1%) and calculate $\bar{\phi}_p$, the average volume fraction of the solute along B5 boundary. Then a test on the solvent mass balance in the truncated part of the tip is performed. Assuming total drying in the tip (there is no more solvent for $y > H$), the solvent mass balance in the truncated tip reads

$$\bar{V}_{tip}(1 - \bar{\phi}_p)\delta = \int_{H-\alpha}^H \frac{J_0}{\sqrt{H-y}} dy = 2J_0\sqrt{\alpha}. \quad (10)$$

If the relative error is larger than about 1%, a new value of \bar{V}_{tip} is tried.

COMSOL software is used to solve the above equations. Preliminary tests were performed to determine the domain size consistent with the assumptions used in the model. For the following results, $H = 5\text{mm}$, $\alpha = 50\mu\text{m}$, $\delta = 2.5\mu\text{m}$ and the viscosity and the diffusion coefficient are $\mu = 10^{-3}\text{Pa}\cdot\text{s}$ and $D = 2 \cdot 10^{-10}\text{m}^2\text{s}^{-1}$.

The thickness of the dried film is obtained from the numerical results by solving the solute mass balance in the truncated part. We assume that the deposit moves at the substrate velocity V . In the truncated region, the solute flux across boundary 5 (cross section δ) is given by the product $\bar{\phi}_p \bar{V}_{tip} \delta$, and the deposit flux on the moving substrate is equal to $\phi_c V h_d$, where ϕ_c is the compaction volume fraction of the deposit. For simplicity, we assume a completely dry deposit and $\phi_c \simeq 1$ which results in the expression

$$h_d = \frac{\bar{\phi}_p \bar{V}_{tip} \delta}{V}. \quad (11)$$

3 Results

3.1 Flow field and concentration distribution

Figure 2 shows the general behavior of the concentration and flow fields corresponding to the conditions $V = 5\mu\text{m/s}$, $v_{ev} = 0.78\mu\text{m/s}$, $\phi_{p0} = 8\%$. The figure on the left is a zoom in the upper part of the domain near the meniscus free surface. The figure on the right is a zoom in the bottom part of the domain where fully developed flow is observed, as expected. For this configuration, we obtain at the boundary B5 $\bar{V}_{tip} = 51.6\mu\text{m/s}$ and $\bar{\phi}_p = 26\%$. As can be seen, a small downward flow is observed

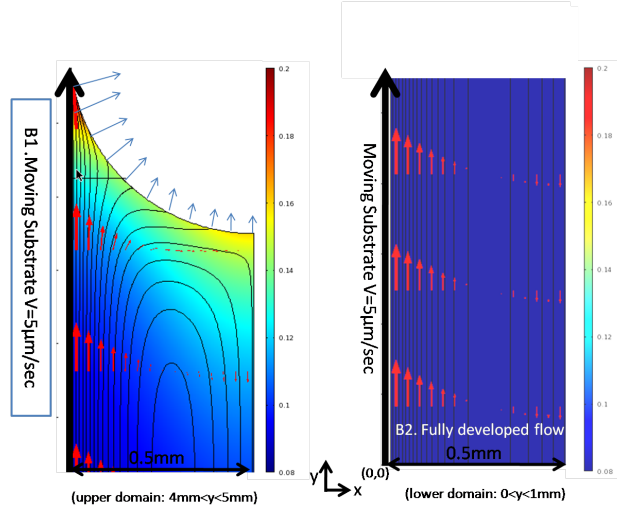


Fig. 2. Numerical results corresponding to $V = 5\mu\text{m/s}$, $v_{ev} = 0.78\mu\text{m/s}$, $\phi_{p0} = 8\%$. Left: an upper part of the domain ($4\text{mm} < y < 5\text{mm}$). Right: a lower part of the domain ($0\text{mm} < y < 1\text{mm}$) with a fully developed flow. Grey levels (color levels online) show the solute volume fraction (0.08 for dark grey at the bottom of the domain (dark blue color online), 0.15 for light grey (yellow color online)). The streamlines and the arrows correspond to the velocity field (u, v) .

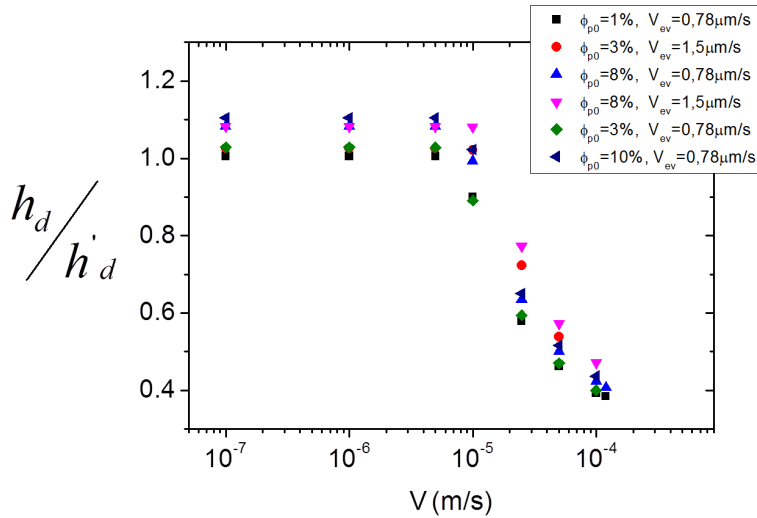


Fig. 3. The ratio of the deposit thicknesses obtained with the 2D model and the simplified model (Eq. (12)).

in the bulk. We notice that it becomes more important for a larger substrate velocity V . It is only for lower velocities that the flow induced by evaporation overcomes that induced by the substrate movement, so that no downward flow is observed (not shown).

3.2 Dry thickness: comparison with a simplified model

As already said in the introduction, this model is a first step and takes into account the substrate motion and evaporation flux only. In the framework of these assumptions, it is interesting to analyze the effect of the downward flow on the deposit thickness at a high substrate velocity. To do so, the deposit thickness is compared to a simple model first proposed by Dimitrov and Nagayama[1] and based on global mass balances. This model assumes a uniform concentration in the cross section L_y ($y = \text{constant}$). The total flux going through L_y is then either evaporating through the meniscus (solvent) or depositing on the substrate at the tip part (solute). We then obtain (see [1,4] for more details)

$$h'_d \simeq \frac{d v_{ev} \phi_{p0}}{2 V} \quad (12)$$

Figure 3 shows the ratio of the thicknesses obtained with numerical simulation to the thickness calculated with the simplified model (estimated with $L_y = B2$), for different evaporation rates and solute concentrations. h_d/h'_d is close to 1 at low velocities, but significantly decreases at velocities larger than $10\mu\text{m}/\text{s}$. As already mentioned, Eq. 12 assumes a uniform solute volume fraction when computing the solute flux across the bottom boundary B2. The effect of this approximation on the estimation of the solute flux is small at $V = 10\mu\text{m}/\text{s}$ (8%), while it is much larger at $V = 100\mu\text{m}/\text{s}$ (138%), and thus the Dimitrov and Nagayama's model does not apply anymore. Indeed, in the case $V = 100\mu\text{m}/\text{s}$, the simulation shows a significant downward flow at a solute concentration higher than the bulk one which means that a significant volume of solute is carried back to the reservoir. Indeed the length needed to homogenize the concentration through diffusion across the cell is much larger than the total height of the Hele-Shaw cell.

However, available experimental data obtained with a dip-coating-like set-up [3–5] do not show this departure from the Dimitrov and Nagayama's model. Several assumptions may be put forward to explain the discrepancy between the experiments and the above simulations. First, it could be due to an insufficient resolution in deposit thickness measurements. Second, this phenomenon takes place at rather high velocities, close to the transition between the evaporative regime and the Landau-Levich regime, and could be overridden by the resulting increase of the thickness. Finally, we also can expect that convection induced by density or surface tension gradients, observed in some experiments but not taken into account in the model, could improve the mixing and thus modify the concentration field, with an impact on the deposit thickness.

4 Conclusion

We proposed a hydrodynamic model of a receding and evaporating meniscus in a dip-coating-like experiment. The difficulties arising from the presence of a contact line are avoided by truncating a small region close to the contact line. The resulting boundary conditions are written using lubrication approximation and mass balances on the truncated domain. In the first step presented in this study, the substrate motion and evaporation are taken into account but buoyancy and Marangoni effect are disregarded. In the framework of these assumptions, large substrate velocities induce a downward flow that carries the solute back to the reservoir. As experimental results do not confirm this result, further investigations are needed to study how hydrodynamic instabilities may modify the concentration field. In a future work, this model will be used as the basic state for a study of the hydrodynamic instabilities in a dip-coating process.

References

1. A.S. Dimitrov and K. Nagayama, *Langmuir*, **12**, (1996) 1303-1311
2. G. Berteloot, C. T. Pham, A. Daerr, F. Lequeux and L. Limat, *Europhys. Lett.*, **83**, (2008) 14003
3. M. Le Berre, Y. Chen and D. Baig, *Langmuir*, **25**, (2009) 2554-2557
4. G. Jing, H. Bodiguel, F. Doumenc, E. Sultan and B. Guerrier, *Langmuir*, **26**, (2010) 2288-2293
5. M. Faustini, B. Louis, P.A. Albouy, M. Kuemmel and D. Grosso, *J. Phys. Chem. C*, **114**, (2010) 7637-7645
6. F. Doumenc and B. Guerrier, *Langmuir*, **26**, (2010) 13959-13967
7. R.D. Deegan, O. Bakajin, T.F. Dupont, G. Huber, S.R. Nagel and T.A. Witten, *Phys. Rev. E*, **62**, (2000) 756-765